npj Ocean Sustainability

https://doi.org/10.1038/s44183-026-00202-4

Article in Press

Offshore wind farms reshape ocean stratification and productivity differently in the North Sea and the Baltic Sea

Received: 21 November 2025

Accepted: 28 April 2026

Cite this article as: Maar, M., Schourup-Kristensen, V., Mohn, C. *et al.* Offshore wind farms reshape ocean stratification and productivity differently in the North Sea and the Baltic Sea. *npj Ocean Sustain* (2026). https://doi.org/10.1038/s44183-026-00202-4

Marie Maar, Vibe Schourup-Kristensen, Christian Mohn, Ange P. Ishimwe, Eva Friis Møller, Charlotte H. Clubley, Andrea N. Hahmann, Marc Imberger & Janus Larsen

Offshore wind farms reshape ocean stratification and productivity differently in the North Sea and the Baltic Sea

Marie Maar[1*], Vibe Schourup-Kristensen[1], Christian Mohn[1], Ange P. Ishimwe[1], Eva Friis Møller[1], Charlotte H. Clubley[1], Andrea N. Hahmann[2], Marc Imberger[2], and Janus Larsen[1]

1) Aarhus University, Department of Ecoscience, Frederiksborgvej 399, 4000 Roskilde, Denmark
2) DTU Wind and Energy Systems, Frederiksborgvej 399, 4000 Roskilde, Denmark

*corresponding author: Marie Maar, e-mail mam@ecos.au.dk

Abstract (150 words)

Planned large-scale offshore wind developments in the North and Baltic Seas are set to transform these regions into major energy hubs for northern Europe. Offshore wind farms are expected to influence the marine ecosystem through two mechanisms: a wind wake effect inducing increased stratification, and a drag effect increasing mixing around monopiles. We applied 3D numerical models that, for the first time, resolve both atmosphere-controlled wind wake effects and monopile drag to quantify their combined impacts on stratification and primary production. The North Sea showed spatially heterogeneous changes, whereas the Baltic Sea exhibited stronger stratification and reduced primary production driven by the wake effect. At current speeds >0.25 m s^{-1}, drag-induced mixing dominated over wake-driven stratification in both seas. The provided knowledge that ecological effects of offshore wind farms depend on prevailing current speeds and baseline stratification can be used to minimize impacts on the environment in future spatial planning.

Introduction

Global warming is projected to have severe impacts on marine ecosystems and the services they provide to human well-being, such as climate- and nutrient regulation, food security, and recreation [1, 2]. Transitioning from fossil fuels to renewable energy can contribute to reductions of greenhouse gas emissions and mitigate climate change impacts on marine ecosystems [3]. Over the past decade, offshore wind farm development has increased substantially due to technological advances, reduced costs, and competitive pricing compared to fossil fuels [3]. Globally, offshore wind farm areas are projected to increase up to 13-fold by 2030, with the largest development expected in northern Europe (36% of total) and Asia (22% of total) [4]. While operating offshore wind energy is a crucial part of Europe's transition to renewable energy sources, its sustainability depends on acceptable impacts on the marine environment. Therefore, there is an urgent need to assess and predict effects of offshore wind on marine species, habitats, and ecosystem functioning [5].

Offshore wind farms are expected to influence the physical and biogeochemical environment through two mechanisms: changes in wind stress at the sea surface (wake effect) and increased friction (drag effect) around monopiles (Figure 1). Offshore wind farms extract kinetic energy from the atmospheric flow, which reduces the wind speed in their wake [6, 7]. The wake effect causes a reduced wind stress at the sea surface and can, for example, lead to less turbulent mixing, change current circulation, change stratification intensity and pattern, and reduce bottom stress [8, 9]. The second mechanism, the drag effect, is increased friction and turbulence from the monopiles, leading to more local turbulent mixing of the water column and changes in current speed [10, 11]. Previous modelling studies have shown that the observed effects not only occur inside wind farms, but also on a regional scale many kilometers away [12-14]. The combined effect of wind wakes and monopile drag on hydrodynamics is therefore a complex interaction, both spatially and temporally, making it difficult to predict the outcome on the marine environment. Regional 3D numerical modelling of hydrodynamics and biogeochemistry is therefore a suitable tool to assess the impacts of offshore wind farm development in different types of marine ecosystems. However, to date no model study on offshore wind farms has included the combined effects of monopile mixing and a fully resolved atmospheric wake extent on both hydrodynamics and biogeochemistry (Table 1).

For northern Europe, the North Sea is designated to become a major renewable energy hub according to the Ostend Declaration of Energy Ministers (The Ostend Declaration.pdf), supporting Europe's strategy to be carbon neutral by 2050. The ambitious target is to increase offshore wind capacity to 120 GW by 2030 and >300 GW by 2050. In the neighboring Baltic Sea, Denmark and Germany cooperate on the Kriegers Flak wind farm and the Bornholm Energy Island. The North Sea and the Baltic Sea differ significantly with respect to morphology, hydrodynamics, and ecological conditions and are therefore expected to respond differently to offshore wind. The North Sea is a highly dynamic shelf-sea dominated by tidal, wind and density driven currents, coastal mixing, seasonal stratification in the deeper parts and large freshwater sources [15]. The southern part is the most productive and characterized by tidal fronts [15]. The Baltic Sea is one of the largest estuaries in the world characterized by a permanent halocline in deeper areas, a seasonal thermocline, high nutrient inputs from the catchment, and limited water exchange with the North Sea. The Baltic Sea is prone to eutrophication with hypoxia, algae blooms, and low water clarity every summer [16]. In both seas, changes in the physical and biogeochemical patterns due to offshore wind may have effects on marine life in terms of changes in the timing and availability of food and habitat suitability [5, 17].

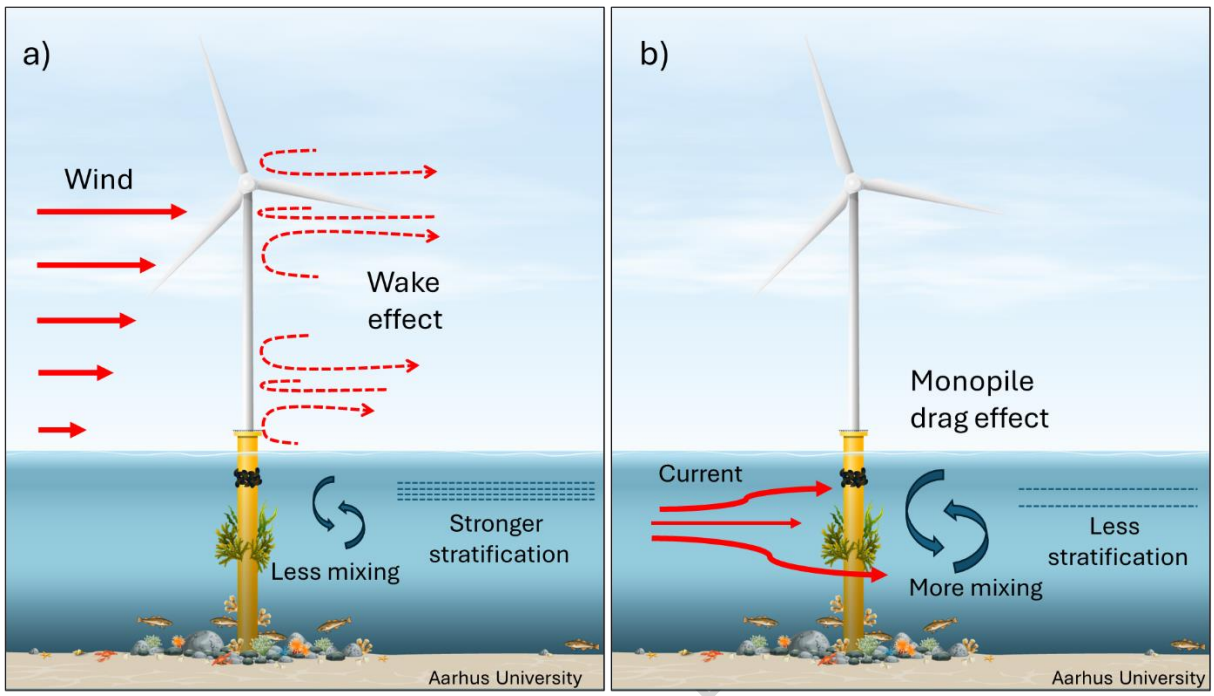

Figure 1. Offshore wind farm effects on hydrodynamics. The effects considered are a) the wind wake causing reduced wind stress at the sea surface, less mixing and stronger stratification of the water column and b) the drag effect from monopiles causing increased local mixing and less stratification of the water column. Hence, the two effects from offshore wind are causing opposite effects on water column mixing and stratification operating on different temporal-spatial scales.

In the North Sea, previous model studies demonstrated changes of physical conditions such as current velocity, water column stratification, bottom stress, salinity, and temperature due to offshore wind [8, 11, 18-21]. These physical changes were found to influence the spatial-temporal distributions of nutrients, phytoplankton, primary production and oxygen potentially leading to changes in the ecological state and productivity [18, 19, 21]. In the Baltic Sea, a model study predicted that expansion of wind power would cause shallowed stratification and changes in deep water salinities [10, 22], but there are until now no studies on the impact on biogeochemistry.

Stratification and primary production are important ecosystem indicators and showed some of the strongest responses to offshore wind farm development in previous studies [5, 18, 23]. Stratification plays a critical role in regulating nutrient transport from the bottom layers to the nutrient-depleted surface, thereby influencing phytoplankton productivity. Increased stratification can lead to an earlier onset of the spring phytoplankton bloom and alter its temporal overlap with zooplankton grazing. Changes in water column stratification are recognized as a key factor in predicting shifts in the abundance of marine species across trophic levels, from lower levels such as sandeel larvae to higher levels including harbor porpoises and black-legged kittiwakes [23]. Consequently, variations in stratification can reveal subtle spatial and seasonal changes within specific habitats, highlighting its value as an indicator of physical processes that shape the entire trophic structure and overall ecosystem functioning [23]. Primary production, closely linked to ecosystem structure and function, serves as an essential indicator of changes in energy flow within the marine food web [24, 25].

In the present study, we evaluate the impact of projected future (year 2030) distributions of offshore and onshore wind farms in two basins, the North Sea and the western Baltic Sea. The future scenario (Y2030) is defined by the Danish Energy Agency [26, 27]. We apply 3D atmospheric model data for the wind wake extent, including realistic wind farm distributions, real turbine sizes, and monopile drag in the 3D coupled hydrodynamic-biogeochemical FlexSem model. The changes in stratification and primary production are compared to a reference scenario (REF-NO-FARM) without any onshore and offshore wind farms. The present model simulations demonstrate that offshore wind farms reshape stratification and primary production differently in the North Sea and Baltic Sea depending on the prevailing current speeds and stratification level. The wake effects inducing stratification are shown to dominate over the monopile mixing effects at current speeds above 0.25 m s^{-1} and the impact range is up to 60 km in both seas. The new knowledge of ecological effects of offshore wind farms can be used to minimize impacts on the environment in future marine spatial planning in the two study areas as well as in other sea basins.

Table 1. Overview of previous model studies of large-scale offshore wind farm developments. Only model studies using 3D hydrodynamic and/or biogeochemical models within large-scale wind farms (not a single turbine) are included. Monopile drag was parameterized either on a sub-grid scale (coarse resolution) or on the scale of individual turbines (dry cells in high resolution). N/A= not assessed.

Area	Hydrodynamic model	Wind wakes	Wind farm capacity (GW)	Monopile drag	Biogeo-chemistry	Reference
North Sea – W Baltic Sea	FlexSem	Interactive 3D atmospheric model	158	Sub-grid scale	ERGOM-FlexSem	Present study
North Sea	ECOSMO	Interactive 3D atmospheric model	120	None	ECOSMO	Daewel et al. 2022
U.S. NE shelf	NS-FVCOM	Interactive 3D atmospheric model	1	Individual turbines	-	Chen et al. 2024
U.S. NE shelf	SCOAR	Interactive 3D atmospheric model	17	None	-	Seo et al. 2025
U.S. California coast	ROMS	Interactive 3D atmospheric model	8.8	None	-	Raghukumar et al. 2023
North Sea	SCHISM	Simplified empirical wake model	N/A	Sub-grid scale	-	Christiansen et al. 2026
North Sea	SCHISM	Parameterized from satellite data with constant wake extent	N/A	None	-	Christiansen et al. 2022
Baltic Sea	NEMO-NORDIC	Max. 8% reduction of wind speed, exp. decay function	N/A	Sub-grid scale	-	Arneborg et al. 2024
North Sea	3D-DCSM-FM	Constant 10% reduction of wind speed inside wind farms, no wake	200	Sub-grid scale	DELWAQ	van Duren et al. 2021
North Sea	3D-GETM-ERSEM-BFM	Constant 10% reduction of wind speed inside wind farms, no wake	N/A	None	ERSEM-BFM	Van den Molen et al. 2014
NW North Sea	FVCOM	Maximum 10% reduction of wind speed, 30 km fixed wake	N/A	None	ERSEM	Zampollo et al. 2025
German Bight (North Sea)	SCHISM	None	N/A	Sub-grid scale and individual turbines	-	Christiansen et al. 2023
Zhoushan Island	Thetis	None	7	Sub-grid scale	-	Zhang er al. 2022
North Sea	SCHISM	None	N/A	Individual turbines	-	Hosseini et al. 2025
SW UK shelf	FVCOM	None	N/A	Individual turbines	-	Cazenave et al. 2016
Baltic Sea	GETM	None	N/A	Sub-grid scale	-	Rennau et al. 2012

Results and Discussion

Offshore wind farm scenario.

An increasing body of work investigates large-scale wind farm impacts on the marine environment, with most studies in the North Sea [11, 12, 18-21, 28]. Only a few studies exist for the Baltic Sea [10, 22], the U.S. northeast coast [29-31] and China [32, 33]. The simulated changes depend on the model parameterizations and future projections of the large-scale wind farm development, which varied among studies (Table 1). The wind-wake effects at the sea surface were represented either by a simple empirical formulation, by outputs from an interactive 3D atmospheric model, or not included. Furthermore, monopile drag effects on hydrodynamics were either implemented as sub-grid scale parameterizations, represented as dry cells for each turbine, or ignored altogether. Finally, many studies considered only hydrodynamic impacts without addressing biogeochemical processes (Table 1). The different model scenarios (number, size, and locations of offshore wind farms) reflect ongoing planning and consultancy processes in the respective countries.

The present study investigates the impact of offshore wind farm developments on stratification and primary production using a 3D coupled hydrodynamic-biogeochemical model including both the wind wake and the monopile drag effects on hydrodynamics. We compare a scenario for windfarms in 2030 (Y2030) with a reference scenario without any wind farms (REF-NO-FARM). In the Y2030 scenario in our study, offshore wind farms are projected to increase to 158.0 GW and the onshore wind farm capacity to 50.4 GW by year 2030 in comparison to a reference scenario without any wind farms [27, 34]. The wake effects calculated by the atmospheric model cause a mean wind speed reduction of up to 2 m s^{-1} with highest impact inside the offshore wind farm areas (Figure 2). The wake effects are stronger in the North Sea than in the Baltic Sea due to the higher wind farm capacity (Figure 2, Supplementary Figure 1 and Supplementary Table 1).

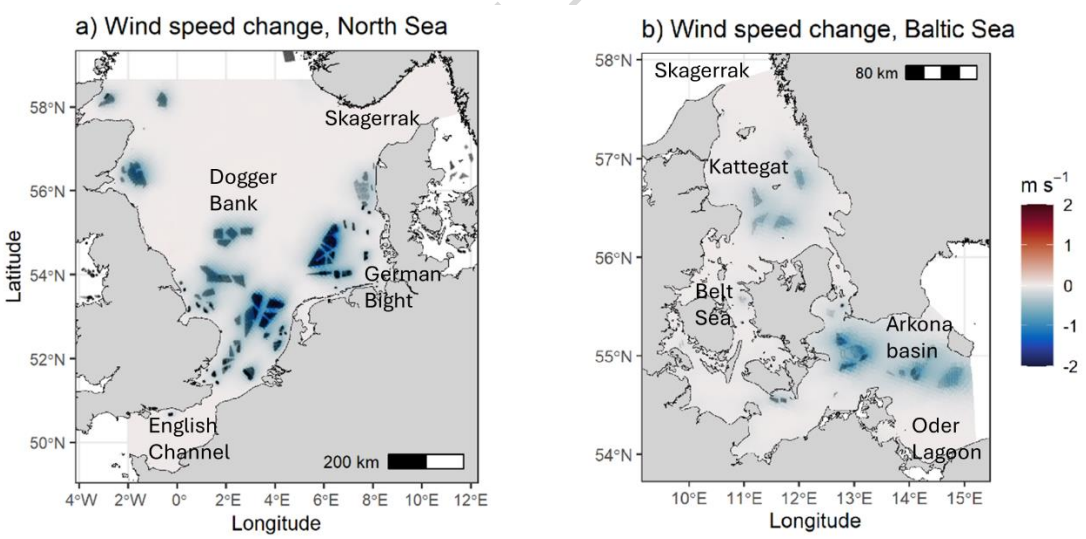

Figure 2. The wake effect (wind speed) around the offshore wind farms. Annual difference in mean wind speed (m s^{-1}) between Y2030 and REF-NO-FARM for a) the North Sea and b) the Baltic Sea from the WRF model. The location of offshore wind farms is shown as black points.

Environmental conditions.

The North Sea and the western Baltic Sea differ markedly in the magnitude of water column stratification, current velocities, and primary production (Figure 3). Stratification is quantified using the Potential Energy Anomaly (PEA, J m^{-3}), which represents the amount of energy required to fully mix the water

column [35]. A water column is considered fully mixed at PEA <1 J m^{-3} and becomes increasingly stratified as PEA values rise. In the North Sea, projected offshore wind farm locations are predominantly situated in mixed or weakly stratified waters, characterized by a mean (±standard deviation, SD) PEA of 11 ± 8 J m^{-3} and mean (±SD) horizontal surface current speeds of 0.28 ± 0.18 m s^{-1} (Figure 3a, c). In contrast, future offshore wind farms in the western Baltic Sea are primarily located in more stratified waters, with a mean (±SD) PEA of 42 ± 29 J m^{-3} and lower mean (±SD) surface current speeds of 0.10 ± 0.08 m s^{-1} (Figure 3b, d). In both seas, seasonal stratification occurs from April to September (Figure 4c, d). The seasonal pattern of depth-integrated primary production starts in February-March and ends around November in both seas (Figure 5c, d). Mean (±SD) primary production within offshore wind farm areas is higher in the North Sea (257 ± 117 mg m^{-2} d^{-1}) compared to the western Baltic Sea (186 ± 59 mg m^{-2} d^{-1}) (Figure 3e, f). Together, these differences highlight the distinct physical and biological environments in which offshore wind farms will operate, with important implications for how turbines may interact with local hydrodynamics and ecosystem functioning.

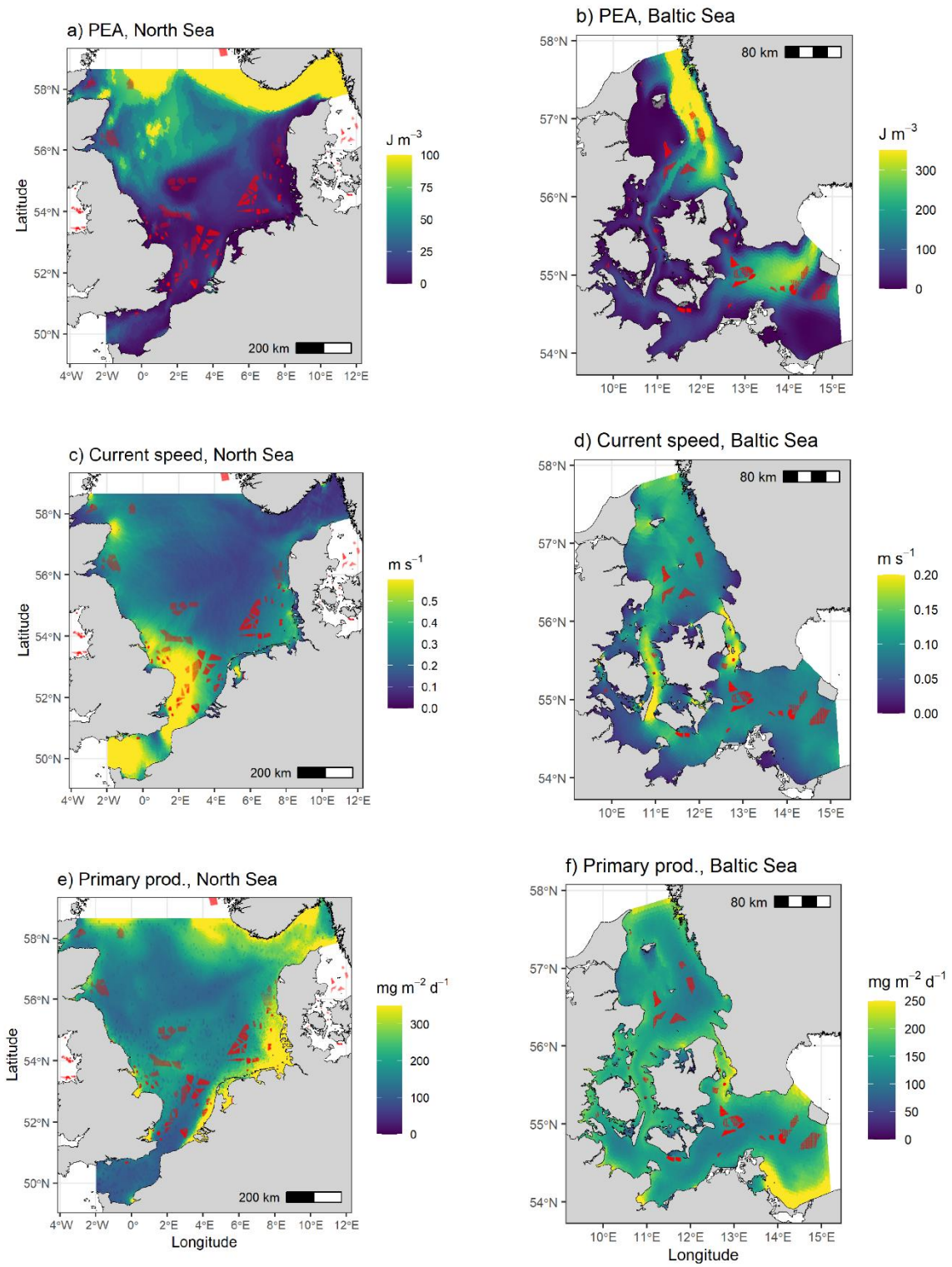

Figure 3. **Stratification, current speed and primary production.** Yearly means of water column stratification index (J m^{-3}) (a, b), current speed (m s^{-1}) (c, d) and primary production (mg-C m^{-2} d^{-1}) for the North Sea and the Baltic Sea, respectively, in the REF-NO-FARM scenario. Maximum PEA was 1019 J m^{-3} and 577 J m^{-3} for the North Sea (Skagerrak) and Baltic Sea (Kattegat), respectively. The location of offshore wind farms is shown as red points.

Impact range of offshore wind farms.

In the North Sea, water column stratification exhibits a dome-shaped spatial pattern, with the most pronounced increase occurring within a 20–60 km radius of offshore wind farms. This enhancement is primarily attributed to wake-induced effects generated by the turbines (Figure 4a), though may also in part result from cumulative effects of nearby wind farms, which were not excluded in these calculations. Beyond this range, stratification gradually declines due to weaker wake effects. In contrast, localized mixing processes driven by monopile structures reduce stratification within the wind farm areas. The zone extending up to 40 km from the farms is influenced by both local monopile mixing and wake effects, with the latter becoming increasingly dominant with distance. Concurrently, primary production increases within the wind farms and gradually diminishes with increasing distance (Figure 5a). This enhancement in annual and summer (April to September) productivity is presumably driven by vertical nutrient transport facilitated by monopile-induced mixing, followed by lateral nutrient dispersion to adjacent regions.

In the western Baltic Sea, changes in stratification peaks within a 10–20 km radius and then progressively decline, stabilizing at approximately 60 km from the wind parks, both annually and during summer (Figure 4b). Inside the offshore wind farms, stratification increases in contrast to the North Sea. The intensified stratification by offshore wind farms is associated with reduced vertical nutrient flux, resulting in lower primary production during summer in contrast to the North Sea (Figure 5b). The estimated impact range of around 60 km in both seas is in agreement with previous studies of atmospheric wakes extending on scales of 55 km and beyond, depending on atmospheric stability [36, 37]. Overall, local monopile-induced mixing is more pronounced in the North Sea than in the western Baltic Sea, creating a transition zone where mixing effects gradually shift to wake-dominated dynamics, extending up to 40 km from offshore wind farms.

Seasonal impacts of offshore wind farms.

For investigation of seasonal effects, a radius of 40 km and 20 km from the offshore wind farms was chosen for the North Sea and the western Baltic Sea, respectively. These radii represent the strongest response of PEA outside the offshore wind farms (Figure 5a, b). The stratification responses to offshore wind farms are most pronounced during summer compared to the annual average, reflecting the reduced influence of wind-driven mixing during this period (Figure 4a, b). In winter, strong wind mixing both in the North Sea and the western Baltic Sea tends to homogenize the water column, thereby dampening stratification signals.

In the North Sea, stratification dynamics inside offshore wind farms exhibit high daily variability, alternating between mixing and stratification events (Figure 4e, Table 2). Outside the wind farms, stratification generally increases from May to September, indicating a seasonal intensification of the wake effect (Figure 4e). This variability mirrors different stratification conditions and is likely driven by the interplay of tidal forcing, large-scale density and wind-driven currents, and coastal mixing processes. In contrast, the western Baltic Sea shows a consistent trend toward stronger stratification across all days, with the most pronounced signal observed inside the offshore wind farm areas (Figure 4f, Table 2).

The daily variability in PEA responses during summer was always lower than the natural daily variability expressed as the coefficient of variation (%) in the reference run (no wind farms) in both sea basins (Table 2). The maximum PEA response was 18.8% inside the offshore wind farms in the western Baltic Sea and comparable to the natural variability of 28.2% (Table 2). Overall, the wake-induced stratification appears to be more dominant than the local mixing effect in the western Baltic Sea, whereas in the North Sea, the two processes are more balanced.

The impact of offshore wind farms on primary production is most pronounced during summer in both the North Sea and the western Baltic Sea, compared to annual averages (Figure 5a, b). This seasonal amplification reflects the nutrient limitation in the surface layer during summer, allowing stratification effects to more strongly modulate nutrient availability for phytoplankton growth.

In the North Sea, primary production within a 40 km radius of offshore wind farms exhibits high daily variability, with both increasing and decreasing responses (Figure 5e). In contrast, the western Baltic Sea shows lower summer productivity, which is offset by an earlier onset of the spring phytoplankton bloom, thereby extending the overall productive season (Figure 5f). The earlier bloom initiation is linked to reduced vertical mixing below the photic zone, caused by wake-induced stratification. Previous studies showed a reduction in Chl *a* concentrations during the spring bloom due to the wind wake effect in the NW North Sea [28] or due to resuspension of particles in the southern tidal part of the North Sea [19]. The daily primary production responses were below the natural daily variability expressed as the coefficient of variation in the reference run in both sea basins (Table 2). However, minimum responses both outside (-20%) and inside (-27%) the offshore wind farms were close to the natural variability in the western Baltic Sea. Overall, these findings suggest that offshore wind farms influence primary production differently across regions and seasons, with the timing and magnitude of biological responses closely tied to local hydrodynamic and stratification regimes.

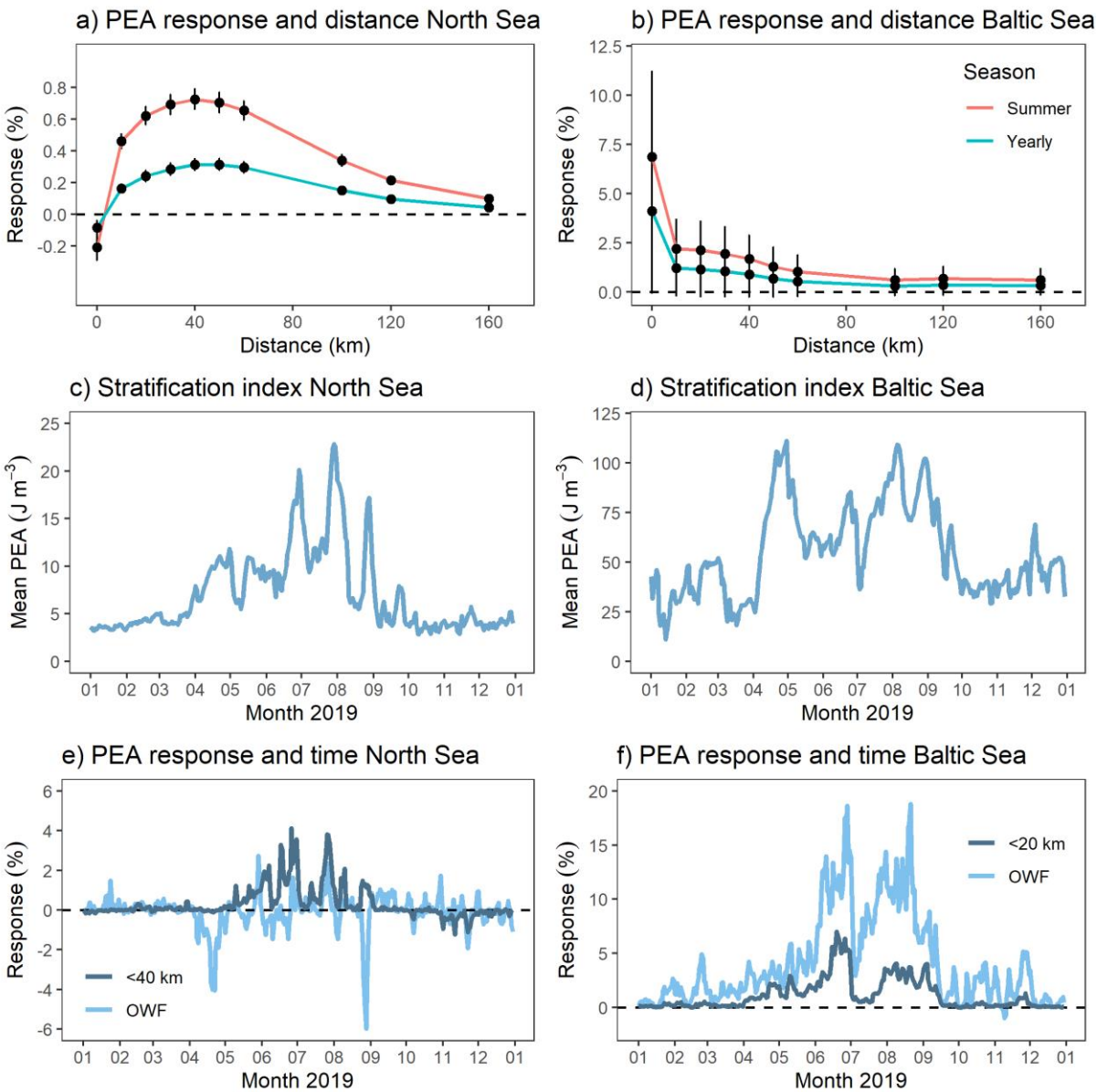

Figure 4. **Stratification index (PEA)**. Mean (±SE) responses of stratification index (%) with increasing distance (km) from the offshore wind farms (a, b) in the North Sea and the western Baltic Sea, respectively, yearly and during summer (April to September). Mean stratification index (J m^{-3}, 0-40 m) within a 40 km radius in the North Sea and 20 km radius in the Baltic Sea from offshore wind farm areas (c, d), and time-series responses of stratification index (%) to offshore wind farm development within the offshore wind farms (OWF) and within a radius of 40 km (North Sea) and 20 km (Baltic Sea) from the OWF (e, f).

Summer	**Min.**	**25th**	**50th**	**Mean**	**75th**	**Max.**	***CV* reference**
Outside wind farms							
North Sea PEA	-0.11	0.06	0.31	0.73	1.23	4.12	40.6
Baltic Sea PEA	0.15	0.90	1.86	2.11	2.93	6.98	26.9
North Sea Prim. prod.	-8.10	0.34	1.08	1.07	1.64	6.94	20.6

Baltic Sea Prim. prod.	-19.7	-2.24	-1.00	-1.72	-0.07	15.6	27.0
Inside wind farms							
North Sea PEA	-5.98	-0.52	-0.01	-0.21	0.29	2.74	40.6
Baltic Sea PEA	0.29	3.13	6.01	6.87	10.5	18.8	28.2
North Sea Prim. prod.	-6.78	0.30	1.19	1.29	2.12	11.0	21.0
Baltic Sea Prim. prod.	-27.2	-7.83	-4.20	-4.84	-1.60	15.2	32.2

Table 2. Summary statistics for daily PEA and primary production responses (%) outside wind farms (<40 km in the North Sea and <20 km in the Baltic Sea) and inside wind farms during summer (Figures 4e,f and 5e,f). Minimum, 25th, 50th and 75th percentiles, mean and maximum values. The coefficient of variation (*CV*; %) is from the reference run without wind farms (April to September).

Annually	**Min.**	**25th**	**50th**	**Mean**	**75th**	**Max.**
North Sea PEA	-17.3	-0.07	0.02	0.21	0.40	18.6
Baltic Sea PEA	-2.92	0.12	0.77	1.39	2.21	10.8
North Sea Prim. prod.	-3.56	-0.04	0.01	0.11	0.14	6.63
Baltic Sea Prim. prod.	-2.56	-0.05	0.00	-0.02	0.07	1.88

Table 3. Summary statistics for annual PEA and primary production responses (%) in the entire North Sea and Baltic Sea (Figure 6). Minimum, 25th, 50th and 75th percentiles, mean and maximum values.

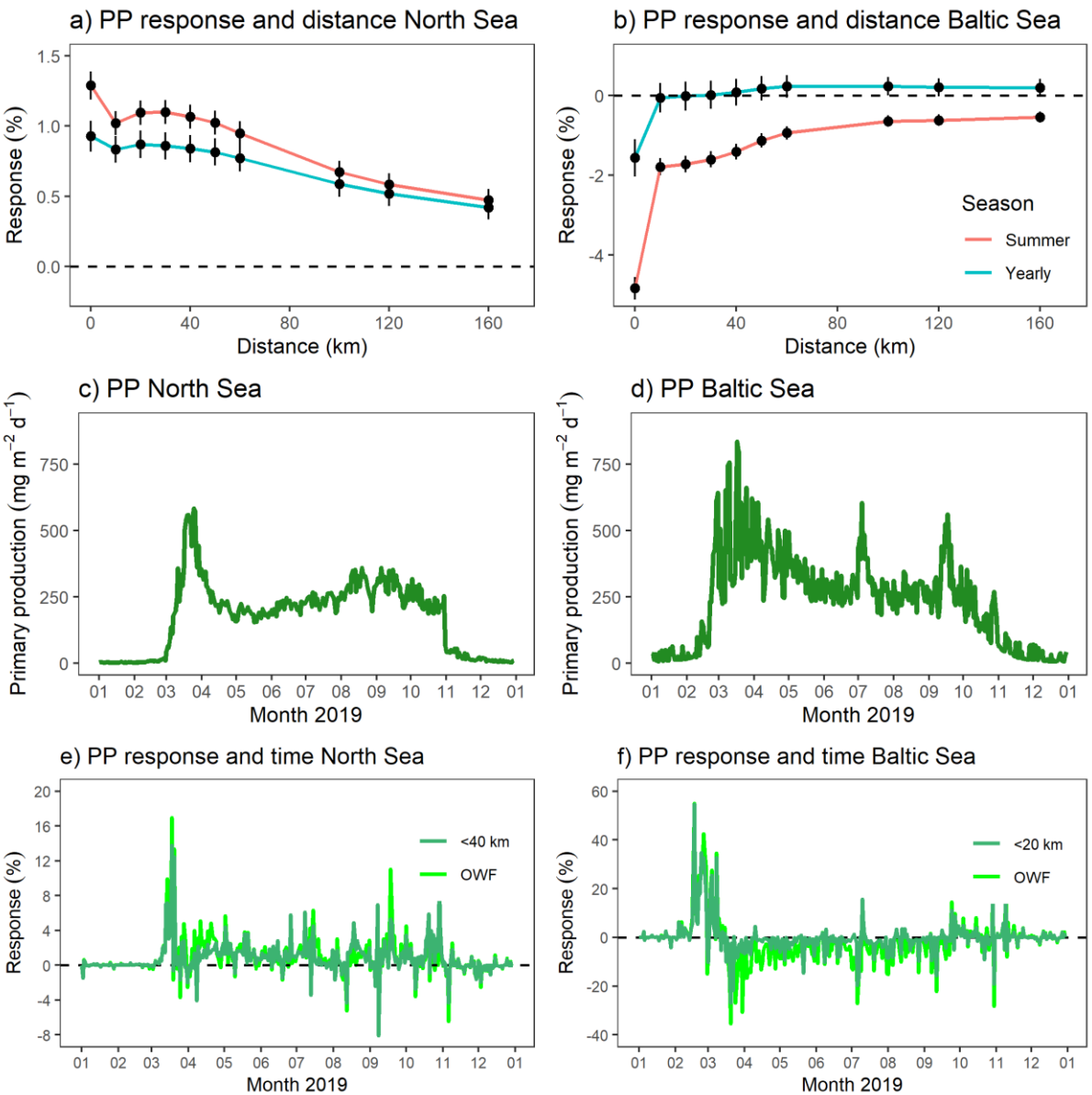

Figure 5. **Primary production**. Mean (±SE) responses of primary production (PP, %) with increasing distances (km) from the offshore wind farms (a, b) in the North Sea and the western Baltic Sea, respectively, yearly and during summer (April to September). Seasonal primary production (mg-C m^{-2} d^{-1}, 0-40 m depth) within a 40 km radius in the North Sea and 20 km radius in the Baltic Sea from offshore wind farms (c, d), and responses of primary production (%) to offshore wind farm development within the offshore wind farms (OWF) and within a radius of 40 km (North Sea) and 20 km (Baltic Sea) from the OWF (e, f).

Spatial impacts of offshore wind farms.

Changes in annual stratification and primary production caused by offshore wind farms exhibit pronounced spatial heterogeneity. In the North Sea, both increases and decreases in stratification and

primary production are observed, resulting in a patchy distribution across the region (Figure 6a, c). Overall, for the North Sea, there was small net increase in stratification and primary production with maximum changes of 18.6% and 6.63%, respectively (Table 3). In the German Bight, where wind farms are numerous, stratification changes are more pronounced due to the cumulative effects of combined wakes. Previous model studies found upwelling and downwelling dipoles with consequences for stratification and productivity in the vicinity of the offshore wind farm clusters in the North Sea [8, 18, 28].

In contrast, the western Baltic Sea displays a more uniform response, with stratification increasing across most of the area and forming smoother spatial gradients (Figure 6b). A previous offshore wind farm model study in the Baltic Sea likewise showed large-scale smooth patterns of temperature and salinity changes [22]. Primary production mainly decreases in the vicinity of the offshore wind farms except for an increase in the south-eastern Kattegat due to local upwelling of nutrients (Figure 6d). Overall, for the western Baltic Sea, there was a small net increase in stratification with a maximum of 10.8% and a small mean decrease of primary production with minimum of -2.56% (Table 3). These differences likely reflect the different current speeds and baseline stratification levels of the two seas.

Overall, monopile mixing effects are found to dominate over the wake effects at mean surface current speeds above 0.25 m s^{-1} causing more mixing in both study areas (Figure 7a). Below this threshold, stratification increases with reduced wind speed as expected (darker red colors in Figure 7a). This relation with wind speed differing between the two basins is probably modified by the different environmental conditions and wind farm capacity. Overall, the response in primary production decreases significantly with increasing stratification response during summer (Figure 7b). However, the pattern shows high variability due to the modification by current speeds (colored symbols in Figure 7b).

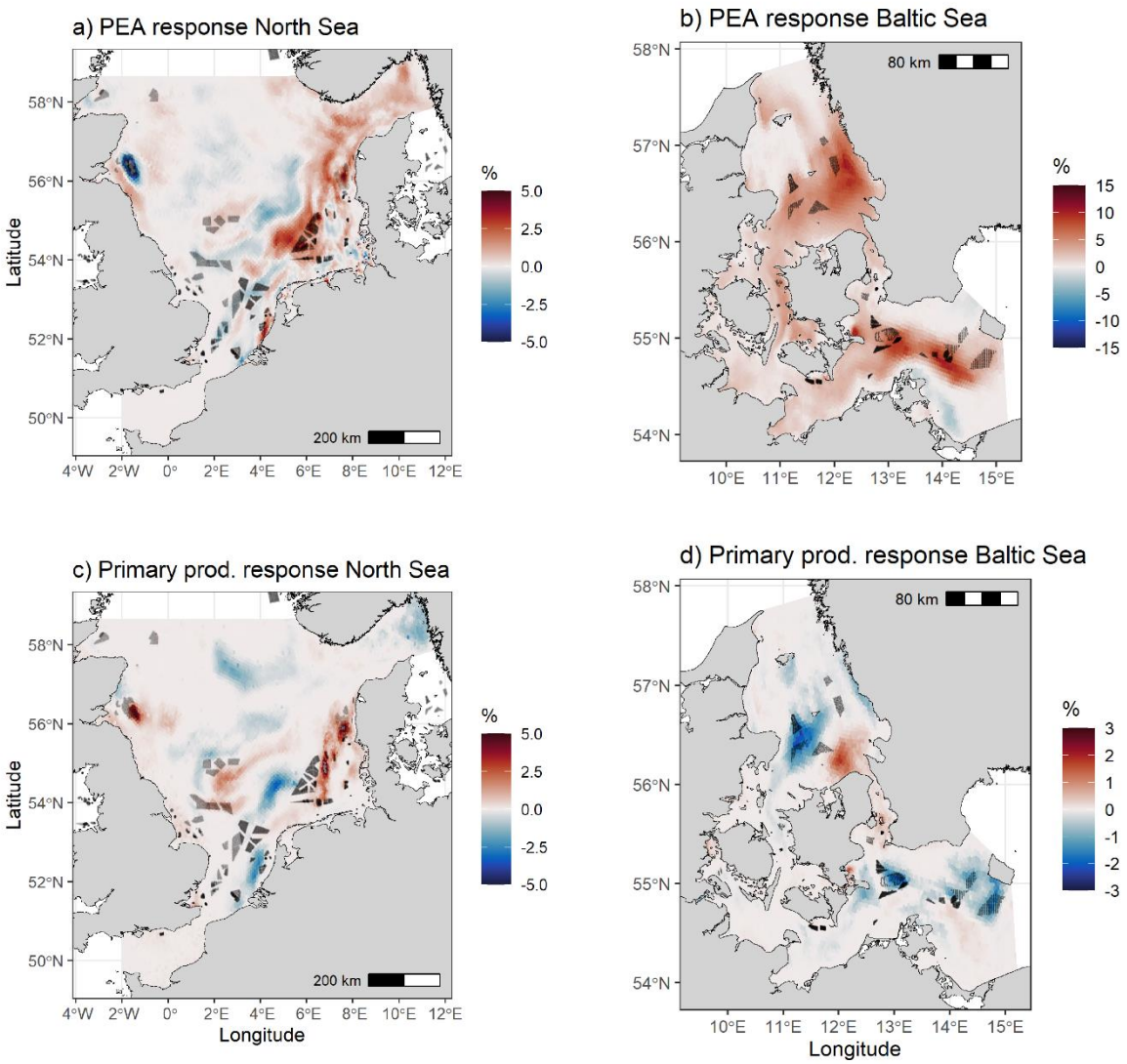

Figure 6. **Spatial responses of stratification and primary production.** Yearly median responses of PEA (a, b) and primary production (c, d) to offshore wind farms for the North Sea and the Baltic Sea, respectively.

Current speeds are generally low (<0.20 m s^{-1}) in areas with stronger stratification response, which corresponded with reduced primary production, as expected (dark blue symbols in Figure 7b). This pattern occurs most of the summer season (Figure 8d). At very high current speeds, there is no response in primary production because the water column is already well mixed (orange symbols in Figure 7b). However, in some areas with intermediate current speeds (0.20-0.25 m s^{-1}) primary production increases with increasing PEA in contrast to the expected pattern. We attribute this deviation to the high variability of the PEA response, which showed the highest SD value of 17 J m^{-3} (Figure 7b). Hence, even though the median PEA increases, the high temporal variability causes stronger intermittent stratification and mixing events favoring primary production (Figure 8b). During periods of more mixing, nutrients are supplied from below, that could be utilized in the following period with increased stratification. The increased stratification could potentially lower the mixing of phytoplankton below the photic zone and thereby contribute to increased primary production. Further, nutrients may be transported laterally from adjacent offshore wind farm areas experiencing increased mixing. In areas where PEA shows a decrease, there is

either an increase in primary production most of the summer period due to the consistent nutrient supply (Figure 8a) or responses in primary production remained low because the water column is already mixed (Figure 8c).

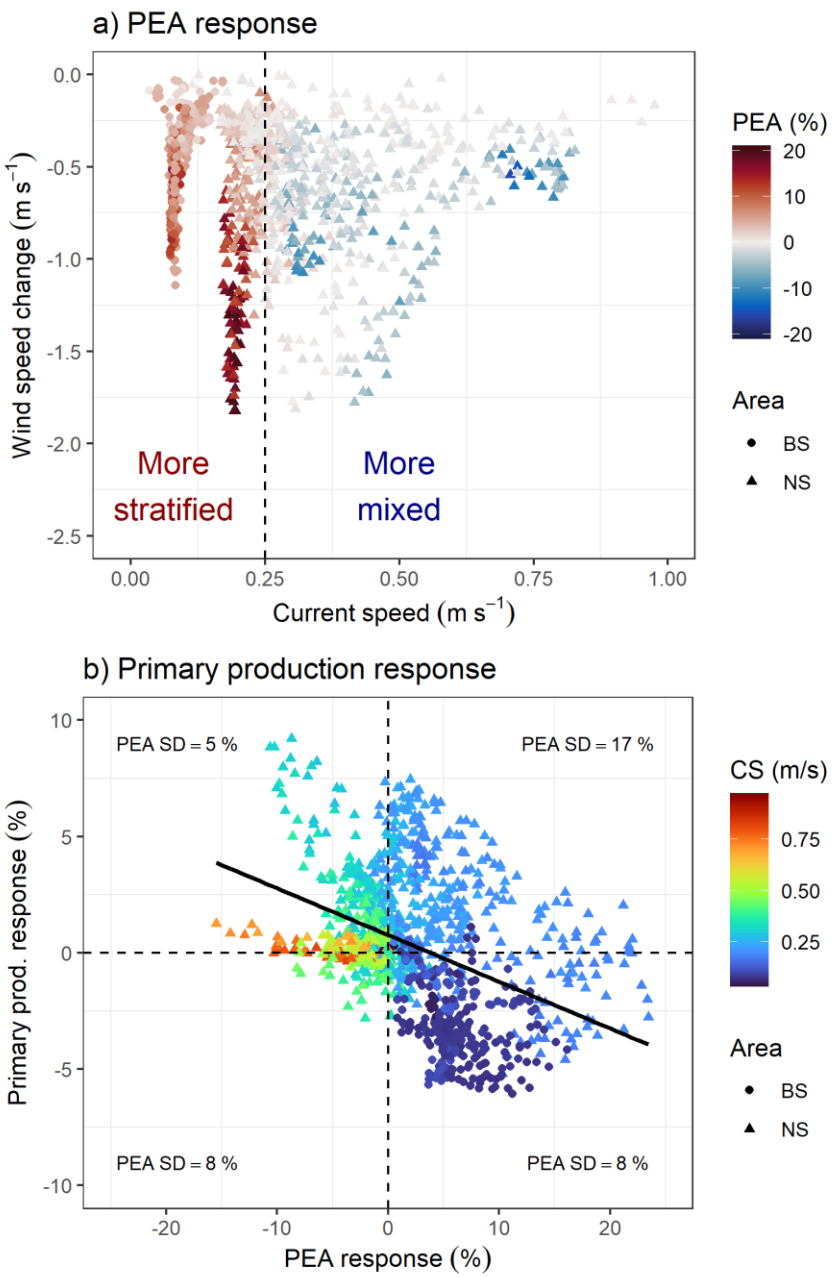

Figure 7. Summer PEA and primary production responses to wind speed and current speed inside the offshore wind farms. (a) Summer PEA response to offshore wind shown as a color scale (%) for wind speed change (y-axis) and mean surface current speed (x-axis). If PEA increases (more stratified), the symbol color is red and if PEA decreases (more mixed), the symbol color is blue according to the color bar. Current speeds >0.25 m s^{-1} indicate

when monopile mixing effects are dominating over the wake effects. Note that the North Sea (848 triangles) and the Baltic Sea (296 circles) have different symbols for the offshore wind farm areas.

(b) Primary production response (y-axis) as a function of PEA response on the x-axis with symbol colors representing mean current speed (CS, m s^{-1}). SD of PEA response (%) within each offshore wind farm area is shown for each box separated by the zero-responses. BS=Baltic Sea, NS=North Sea. There was a significant Pearson correlation between primary production response versus PEA response (black solid line: N=1144, R= -0.40, R^2=0.16, p<0.001). Regression line: Y = -0.20X + 0.76. All the primary production responses (increase or decrease) are further analyzed for PEA responses (increase or decrease) in Figure 8.

Model uncertainties.

The formulation of the wind wakes is based on an interactive atmospheric model with realistic wind farm distributions and real turbine sizes that conceivable is more accurate than the simpler approach applied in other studies (Table 1). Model results have been evaluated against observations [27, 38], but data are limited due to sparse observations, and large wind farms like those planned for 2030 have yet to be constructed. Interpretation of the scenario results can be challenging because the atmospheric forcing includes the wind wake effect from both offshore and onshore wind farms as well as changes in atmospheric temperature and cloud cover [27]. In addition, there is no feedback from the sea to the atmosphere regarding surface fluxes that may affect wind speed and wakes in the atmosphere [39]. Recent studies show that wake–ocean interactions can modify near-surface meteorology and air–sea fluxes, indicating that coupled ocean–atmosphere modeling may be necessary to assess the potential oceanographic impacts of offshore wind farm development [30]. Nevertheless, the role of air–sea interactions mediated by offshore wind farms remains insufficiently understood [30]. Onshore wind farms can also produce wind-wake effects over nearby sea areas, but these impacts are minor compared with those from offshore wind farms, which cause a much stronger reduction in offshore wind speeds (Figure 2).

The formulation of the monopile drag effect depended on the physical shape of the monopiles including epifauna and the scour protection. The applied coefficients are therefore uncertain [11]. Further, while the resolution of the model domain is high, it is relatively coarse in relation to the size of the individual monopiles, and the sub-scale grid parameterization of the monopile effect introduces uncertainties. Due to the large spatial extent and the high number of monopiles in current and future OWFs, explicitly resolving each structure within the mesh is computationally challenging in a basin-scale setup - unlike previous studies focused on smaller domains [11, 29]. Johnson, van Berkel [40], using a Computational Fluid Dynamics (CFD) model to assess combined effects of monopiles and scour protection, reported a higher drag coefficient of 1.035, compared to the value of 0.63 applied in this study [10].

The scenarios are conducted for one standard year, but the effects may accumulate over years until the system gets adjusted to the new impact [22]. Further, assessment of the interannual variations is needed to consolidate the results. Detritus resuspension is included in the model, but resuspension of inorganic particles is missing and could be important for primary production in the tidal areas of the North Sea [19]. At the open boundary between the North Sea and the western Baltic Sea, we assume no change in forcing data from offshore wind farms in the neighboring area. However, far-field effects from offshore wind were shown to be important and could lead to changes across basins [22].

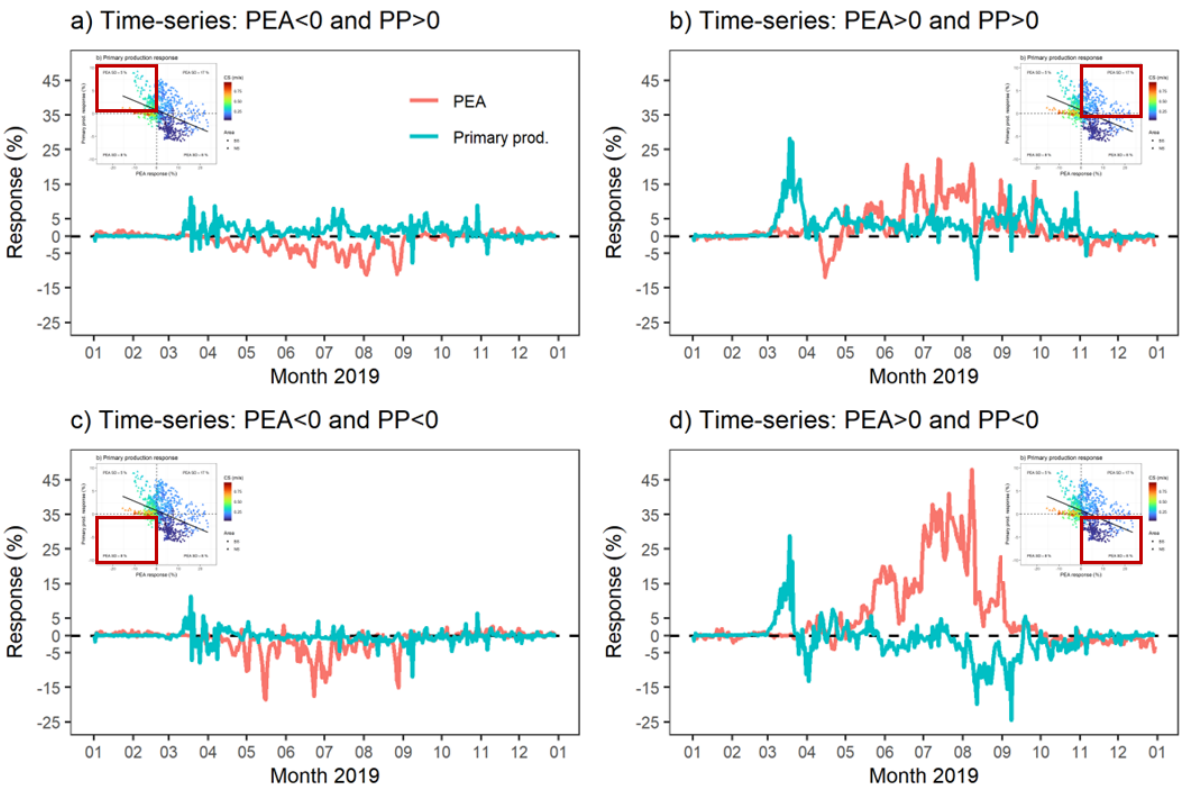

Figure 8. Time-series of PEA and primary production (PP) responses inside the offshore wind farm areas. Summer PEA and primary production were averaged for all wind farms areas according to the four outcomes in Figure 7b: a) Decreased summer PEA and increased summer primary production, b) decreased PEA and increased primary production, c) decreased PEA and decreased primary production, and d) increased PEA and decreased primary production. The inserted subfigures show the extracted data area (red box) in Figure 7b.

Future perspectives.

This modeling study emphasizes the critical need to consider both the wind wake and the monopile drag effects together with the specific hydrodynamic and biogeochemical conditions of an area when evaluating the impacts of offshore wind farms. The results demonstrate that differences in current speeds and stratification between sea basins strongly influence whether stratification and primary production responses increase or decrease. Disentangling the influence of individual wind farms within a complex arrangement of interacting wake and drag effects is inherently challenging. In the present configuration, areas of reduced wind speed and altered circulation overlap, making it difficult to isolate the response attributable to any single installation. Resolving such interactions would require a larger suite of targeted simulations in which wind farms are placed individually and at varying distances from one another. As a next step, modeling experiments could be designed to systematically vary spacing, layout, and upscaling scenarios in order to better distinguish individual from combined effects and to quantify how different configurations shape ecosystem responses.

The wind farm-induced changes in stratification and primary productivity could potentially affect higher trophic levels [41]. In the future, the output of the hydrodynamic-biogeochemical models could be coupled to models of higher trophic levels such as fish, marine mammals, and birds to get a full end-to-end approach of food web effects from offshore wind farm development [42, 43]. Colonizing species on the monopiles, such as mussels and seaweed, may likewise contribute to changes in nutrient cycling, Chl *a* concentrations and carbon deposition [17, 44-46], and these impact could also be included in future model developments.

With global offshore wind farm development projected to increase dramatically [4], there is a growing need for knowledge that minimizes impacts on the marine environment within marine spatial planning processes and environmental impact assessments. This study demonstrates how the interplay between wake effects and monopile-induced mixing alters stratification and primary production across different temporal and spatial scales, highlighting the critical role of current speed in shaping these responses. Although the analysis focuses on the North Sea and western Baltic Sea, the modeling approach and identified key mechanisms can inform assessments in other shelf seas worldwide, providing insights into which processes are likely to be most influential for the marine environment during offshore wind farm development.

Methods

Scenarios

The response of the marine physical and biogeochemical environment to offshore wind farm development was simulated using 3D coupled hydrodynamic-biogeochemical models for the North Sea and the western Baltic Sea. The wind farm scenarios were developed by the Danish Energy Agency and included a reference scenario without any onshore and offshore wind farms (REF-NO-FARM), and a future scenario for 2030 (Y2030) [26, 27, 34]. In Y2030, the offshore wind farm capacity was 158.0 GW and the onshore wind farm capacity 50.4 GW (Supplementary Figure 1).

Meteorological conditions from the year 2019 were used for both scenarios, selected as typical year of the past 30 years based on distribution of wind speed, direction, and atmospheric stability (Supplementary Figure 2). Time-series data was extracted from 15 locations randomly selected within the greater North Sea - Baltic Sea area. Averaged over all locations, the individual years were ranked for each variable based on their similarity to the long-term average (1989– 2021) using the online tool climrepper [47]. 1999 was the most representative year (when weighting wind speed, direction and stability equally) but due to lack of validation data, 2019 was used as the best compromise between atmospheric conditions and the actual availability of measurements. For marine conditions, the monitoring parameters in 2019 also did not show any unambiguous changes in relation to the development in recent years of the marine environment [48].

Model description

Two high-resolution model setups were deployed, one for the North Sea and one for the western Baltic Sea, using the open-source FlexSem framework [49, 50]. FlexSem includes a 3D hydrodynamic model that solves the Navier–Stokes equations on an unstructured mesh with C-grid staggering. The advection-diffusion equation was solved using a second-order total variation diminishing (TVD) advection-diffusion scheme [51]. Turbulence was modelled using a *k*–epsilon model in the vertical [52, 53] and a

Smagorinsky scheme in the horizontal [54]. Surface heat exchange was calculated using a radiation model that modifies water temperature through ocean-atmosphere heat fluxes [49].

Biogeochemistry was simulated using a modified version of the Ecological Regional Ocean Model (ERGOM-AU) implemented in FlexSem, which includes coupled pelagic and benthic components [50, 55]. ERGOM simulates the cycling of nitrogen (N) and phosphorous (P) using Redfield ratios [56, 57]. The 10 state variables describe concentrations of inorganic nutrients (NO_3, NH_4, PO_4), two functional groups of phytoplankton (diatoms, flagellates), micro- and mesozooplankton, detritus, oxygen, and suspension feeders. The model considers the processes of nutrient uptake, growth, grazing, respiration, excretion, recycling, mortality, and settling of detritus and diatoms. In the western Baltic Sea, the biological model was updated to include two classes of dissolved organic nitrogen (DON), a labile class with fast turnover and a refractory class with slower turnover [58].

The Greater North Sea model (OSPAR Region II), covers the area from the English Channel in the south to the northern North Sea and Norwegian Trench in the north, extending to the Skagerrak in the northeast (Supplementary Figure 3). Horizontal resolution varied from 7.8 km in the central basin, 3.9 km in the western and coastal regions, to 2.5 km in the Wadden Sea. Vertically, the model used 29 z-layers: ten layers of 5 m, five of 10 m, five of 20 m, and nine of 50 m, reaching a maximum depth of 682 m. Wetting and drying were included to account for tidal variations. Freshwater and nutrient inputs from 121 rivers were included using data from NOVANA [59] and the OSPAR ICG-EMO database [60]. Total nitrogen (TN) was distributed into nitrate (90%), ammonium (2%) and detritus (8%). Phosphate was 48% of total phosphorus (TP). Salinity was zero and temperature the same as in seawater. More details of model set-up and validation can be found in Maar, Schourup-Kristensen [50].

The western Baltic Sea model covered the Inner Danish Waters from Northern Kattegat to the island of Bornholm in the western Baltic Sea (Supplementary Figure 4). The horizontal resolution ranges from approximately 200 meters in the Little Belt, to 5 km in northern Kattegat and the Baltic Sea. In the vertical, the model had z-layers with a resolution of 1 meter and 84 layers. The surface layer was 2 meters thick to accommodate sea surface height fluctuations. The maximum depth was 84.5 meters. Daily freshwater and nutrient runoff data from 76 rivers were obtained from the DK-QNP model [59] and the E-HYPE catchment model [61]. TN was distributed into nitrate (74%), ammonium (2%), DON labile (13%) and DON refractory (11%) and phosphate was 65% of TP [57]. Salinity was zero and temperature the same as in seawater. More details of model set-up and validation can be found in Maar, Schourup-Kristensen [50].

Meteorological forcing (wind, air temperature, cloud cover, specific humidity) was provided by the high-resolution 3D Weather Research and Forecasting WRF model [27, 62, 63]. WRF coupled with Fitch wind farm parameterization [64] models how wind turbines convert atmospheric energy into electricity, reducing downstream wind speed (wake effect) and sometimes increasing side speeds (speed-up effect) [65]. They also generate turbulence through tip vortices and shear, affecting wind, turbulence, temperature, and humidity around wind farms [66]. The wind stress, τ at the sea surface was described as a function of the difference in surface water velocity and 10 m atmosphere velocity [67].

Offshore monopiles providing foundation for marine wind turbines act as physical obstacles, reducing mean currents and increasing turbulence [68]. Their effects were parameterized by adding drag and turbulent kinetic energy [10]. Monopile diameters were set to 7.5 m for turbines <15 MW and 13 m for

turbines ≥15 MW. The drag coefficient was set to 0.63 and the diffusion coefficient was 1.4 representing a "weak mixing" scenario [10].

Model variables and analysis

Stratification, governed by salinity and temperature gradients, limits the vertical exchange of nutrients and oxygen that is important for the biogeochemical processes. The stratification index was calculated as the Potential Energy Anomaly (PEA, J m^{-3}), representing the energy required to mix the water column [35].

Primary production was estimated by multiplying the growth rate of each phytoplankton group by its corresponding biomass and then summing the contributions of the two groups. Depth-integrated primary production was calculated over 0–40 m in the North Sea and 0–20 m in the Baltic Sea. Nitrogen-based biomass (mmol N) was converted to carbon biomass (mg C) using the Redfield C:N ratio of 6.625 and a molar mass of 12 g C mol^{-1}.

The ecosystem variable responses (*VR*, %) were calculated as the difference between the Y2023 scenario (*SCE*) and the REF-NO-FARM scenario (*REF*) divided by the mean of *REF* and multiplied by 100% for each grid cell [18]. *VR* was estimated daily during the phytoplankton productive season (April–September, n = 180 days) and annually. The response was investigated for stratification and primary production for the upper 40 m in the North Sea and upper 20 m in the western Baltic Sea. For the reference run, the coefficient of variation was estimated as $CV = SD/mean * 100\%$ for comparison with natural daily variability during summer.

To determine the impact range of offshore wind farms on PEA and primary production, offshore wind farm point locations were first overlaid on the North Sea and Inner Danish waters model meshes and the model elements containing an offshore wind turbine were identified. For each element containing an offshore wind turbine, a buffer zone of increasing distance (0, 10, 20, 30, 40, 50, 60, 110, 120, 160 km) was applied using the 'st_buffer' function of the 'sf' R package [69]. All model elements that fell within these buffer areas were identified, and for each buffer distance the mean (± SE) response of PEA and PP within these elements was calculated. Wind turbines that fell on land were not included in the calculations of offshore wind impact range.

Data availability

The datasets generated during the current study will be publicly available at Zenodo.org after acceptance.

Code availability

The model source code is published on Zenodo.org [70, 71].

Competing interests

The authors declare no competing financial or non-financial interests.

Acknowledgments

This study was supported by the project “Environmental mapping and screening of the offshore wind potential in Denmark” funded by the Danish Energy Agency, the OLAMUR project funded by the European Union (grant agreement no. 101094065) and the WIN@Sea project funded by the Velux Foundation.

Author contributions

M.M. wrote the main manuscript, conducted the scenario runs, and analyzed the results. J.L. developed the FlexSem model, made the physical model set-ups, implemented the monopile drag formulation and contributed to the writing. V.S.K. validated and implemented the biogeochemical models and contributed to the writing. C.C. supported the analysis, made some of the figures and contributed to the writing. A.I. implemented a new second order advection scheme and improved the wind surface drag formulation. C.M. conducted the physical model validation and contributed to the writing. A.H and M.I. made the wind wake scenarios, provided meteorological forcing data and contributed to the writing. E.F.M. provided funding, ideas and contributed to the writing. All authors reviewed the manuscript.

References

1. Magnan, A.K., et al., *Implications of the Paris agreement for the ocean.* Nature Climate Change, 2016. **6**(8): p. 732-735.
2. Gattuso, J.-P., et al., *Ocean Solutions to Address Climate Change and Its Effects on Marine Ecosystems.* Frontiers in Marine Science, 2018. **5**(337).
3. Galparsoro, I., et al., *Reviewing the ecological impacts of offshore wind farms.* npj Ocean Sustainability, 2022. **1**(1): p. 1.
4. Maar, M., et al., *Multi-use of offshore wind farms with low-trophic aquaculture can help achieve global sustainability goals.* Communications Earth & Environment, 2023. **4**(1): p. 447.
5. Isaksson, N., et al., *A paradigm for understanding whole ecosystem effects of offshore wind farms in shelf seas.* ICES Journal of Marine Science, 2023.
6. Volker, P.J.H., et al., *Prospects for generating electricity by large onshore and offshore wind farms.* Environmental Research Letters, 2017. **12**(3): p. 034022.
7. Ludewig, E., *On the Effect of Offshore Wind Farms on the Atmosphere and Ocean Dynamics*. Hamburg Studies on Maritime Affairs. 2015, https://doi.org/10.1007/978-3-319-08641-5: Springer Cham. 162.
8. Christiansen, N., et al., *Emergence of Large-Scale Hydrodynamic Structures Due to Atmospheric Offshore Wind Farm Wakes.* Frontiers in Marine Science, 2022. **9**.
9. Christiansen, N., U. Daewel, and C. Schrum, *Cumulative hydrodynamic impacts of offshore wind farms on North Sea currents and surface temperatures.* Communications Earth & Environment, 2026. **7**(1): p. 164.
10. Rennau, H., S. Schimmels, and H. Burchard, *On the effect of structure-induced resistance and mixing on inflows into the Baltic Sea: A numerical model study.* Coastal Engineering, 2012. **60**: p. 53-68.
11. Christiansen, N., et al., *The large-scale impact of anthropogenic mixing by offshore wind turbine foundations in the shallow North Sea.* Frontiers in Marine Science, 2023. **10**.
12. Cazenave, P.W., R. Torres, and J.I. Allen, *Unstructured grid modelling of offshore wind farm impacts on seasonally stratified shelf seas.* Progress in Oceanography, 2016. **145**: p. 25-41.
13. Schultze, L.K.P., et al., *Increased Mixing and Turbulence in the Wake of Offshore Wind Farm Foundations.* Journal of Geophysical Research: Oceans, 2020. **125**(8): p. e2019JC015858.
14. Li, X., et al., *SAR observation and numerical modeling of tidal current wakes at the East China Sea offshore wind farm.* Journal of Geophysical Research: Oceans, 2014. **119**(8): p. 4958-4971.
15. van Leeuwen, S., et al., *Stratified and nonstratified areas in the North Sea: Long-term variability and biological and policy implications.* Journal of Geophysical Research: Oceans, 2015. **120**(7): p. 4670-4686.
16. Carstensen, J., et al., *Coastal eutrophication and trend reversal: A Danish case study.* Limnology and Oceanography, 2006. **51**(1): p. 398-408.
17. Maar, M., et al., *Local effects of blue mussels around turbine foundations in an ecosystem model of Nysted off-shore wind farm, Denmark.* Journal of Sea Research, 2009. **62**(2-3): p. 159-174.
18. Daewel, U., et al., *Offshore wind farms are projected to impact primary production and bottom water deoxygenation in the North Sea.* Communications Earth & Environment, 2022. **3**(1): p. 292.
19. van Duren, L., et al., *Eosystem effects of large up-scaling of offshore wind on the North Sea - a synthesis. Deltares.* 2021. p. 1-42.
20. Hosseini, S.T., et al., *Impact of offshore wind farm monopiles on hydrodynamics interacting with wind-driven waves.* Ocean Modelling, 2025. **195**: p. 102521.
21. van der Molen, J., et al., *Predicting the large-scale consequences of offshore wind turbine array development on a North Sea ecosystem.* Continental Shelf Research, 2014. **85**: p. 60-72.

22. Arneborg, L., et al., *Hydrographic effects in Swedish waters of future offshore wind power scenarios. REPORT OCEANOGRAPHY No 77. Department of Research and Development, SMHI.* 2024. p. 1-26.
23. Trifonova, N., et al., *Use of Our Future Seas: Relevance of Spatial and Temporal Scale for Physical and Biological Indicators.* Frontiers in Marine Science, 2022. **Volume 8 - 2021**.
24. Schlenger, A.J., S. Libralato, and L.T. Ballance, *Temporal Variability of Primary Production Explains Marine Ecosystem Structure and Function.* Ecosystems, 2019. **22**(2): p. 331-345.
25. Tomczak, M.T., et al., *Ecological Network Indicators of Ecosystem Status and Change in the Baltic Sea.* PLOS ONE, 2013. **8**(10): p. e75439.
26. Energistyrelsen, *Notat om scenarier for havvindudbygning frem mod 2030.* 2024.
27. Hahmann, A.N., et al., *Environmental Mapping and Screening of the Offshore Wind Potential in Denmark. Sensitivity mapping: Wind, DTU Public report number DTU E-0255 2025*. 2025: https://backend.orbit.dtu.dk/ws/files/400503926/ENSreport_V4.0_1May2025.pdf.
28. Zampollo, A., et al., *Does the oceanographic response to wind farm wind-wakes affect the spring phytoplankton bloom?* Progress in Oceanography, 2025. **237**: p. 103512.
29. Chen, C., et al., *Potential impacts of offshore wind energy development on physical processes and scallop larval dispersal over the US Northeast shelf.* Progress in Oceanography, 2024. **224**: p. 103263.
30. Seo, H., et al., *Sea surface warming and ocean-to-atmosphere feedback driven by large-scale offshore wind farms under seasonally stratified conditions.* Science Advances, 2025. **11**(45): p. eadw7603.
31. Raghukumar, K., et al., *Projected cross-shore changes in upwelling induced by offshore wind farm development along the California coast.* Communications Earth & Environment, 2023. **4**(1): p. 116.
32. Zhang, J., et al., *Interactions between tidal stream turbine arrays and their hydrodynamic impact around Zhoushan Island, China.* Ocean Engineering, 2022. **246**: p. 110431.
33. Liu, K., et al., *Spatiotemporal Variations of Ocean Upwelling and Downwelling Induced by Wind Wakes of Offshore Wind Farms.* Journal of Marine Science and Engineering, 2023. **11**(10): p. 2020.
34. Hahmann, A.N., et al., *Environmental Mapping and Screening of the Offshore Wind Potential in Denmark. Interannual Variability of Wake Effects*. 2025, DTU: https://backend.orbit.dtu.dk/ws/portalfiles/portal/422587458/ENSreport_Interannual_Variability_Final.pdf. p. 21.
35. Simpson, J.H. and D. Bowers, *Models of Stratification and Frontal Movement in Shelf Seas.* Deep-Sea Research Part A-Oceanographic Research Papers, 1981. **28**(7): p. 727-738.
36. Bärfuss, K., J. Schulz-Stellenfleth, and A. Lampert, *The Impact of Offshore Wind Farms on Sea State Demonstrated by Airborne LiDAR Measurements.* Journal of Marine Science and Engineering, 2021. **9**(6): p. 644.
37. Platis, A., et al., *Long-range modifications of the wind field by offshore wind parks – results of the project WIPAFF.* Meteorologische Zeitschrift, 2020. **29**(5): p. 355-376.
38. Fischereit, J., et al., *Modelling wind farm effects in HARMONIE–AROME (cycle 43.2.2) – Part 1: Implementation and evaluation.* Geosci. Model Dev., 2024. **17**(7): p. 2855-2875.
39. Fischereit, J., X.G. Larsén, and A.N. Hahmann, *Climatic Impacts of Wind-Wave-Wake Interactions in Offshore Wind Farms.* Frontiers in Energy Research, 2022. **10**.
40. Johnson, T., et al., *Hydrodynamic modeling, particle tracking and agent-based modeling of larvae in the U.S. mid-Atlantic bight. Lakewood (CO): US Department of the Interior, Bureau of Ocean Energy Management. OCS Study BOEM 2021-049. 232 p.* 2021.
41. Wang, J., et al., *Effects of established offshore wind farms on energy flow of coastal ecosystems: A case study of the Rudong offshore wind farms in China.* Ocean & Coastal Management, 2019. **171**: p. 111-118.

42. van de Wolfshaar, K.E., et al., *Sensitivity of the fish community to different prey fields and importance of spatial-seasonal patterns.* Marine Ecology Progress Series, 2021. **680**: p. 79-95.
43. Bossier, S., et al., *The Baltic Sea Atlantis: An integrated end-to-end modelling framework evaluating ecosystem-wide effects of human-induced pressures.* PLOS ONE, 2018. **13**(7): p. e0199168.
44. De Borger, E., et al., *Offshore Windfarm Footprint of Sediment Organic Matter Mineralization Processes.* Frontiers in Marine Science, 2021. **8**.
45. Voet, H.E.E., et al., *Organic matter processing in a [simulated] offshore wind farm ecosystem in current and future climate and aquaculture scenarios.* Science of The Total Environment, 2023. **857**: p. 159285.
46. Slavik, K., et al., *The large-scale impact of offshore wind farm structures on pelagic primary productivity in the southern North Sea.* Hydrobiologia, 2019. **845**(1): p. 35-53.
47. Imberger, J. and J. Fischereit, *climrepper - A Python package for determining climatological representative periods (v1.0.1). Zenodo. https://doi.org/10.5281/zenodo.15050656*. 2025.
48. Hansen, J. and S. Høgslund, *Marine områder 2019. NOVANA.*, in *Videnskabelig rapport fra DCE - Nationalt Center for Miljø og Energi*. 2021: Aarhus Universitet, DCE - Nationalt Center for Miljø og Energi. p. 174.
49. Larsen, J., et al., *A versatile marine modelling tool applied to arctic, temperate and tropical waters.* PLOS ONE, 2020. **15**(4): p. e0231193.
50. Maar, M., et al., *Spatial impact of offshore wind farms on hydrodynamics and biogeochemical environment. Aarhus University, DCE – Danish Centre for Environment and Energy, 70 pp.* 2025.
51. Wang, Q., et al., *Development of a total variation diminishing (TVD) sea ice transport scheme and its application in an ocean (SCHISM v5.11) and sea ice (Icepack v1.3.4) coupled model on unstructured grids.* Geosci. Model Dev., 2024. **17**(18): p. 7067-7081.
52. Burchard, H., O. Petersen, and T.P. Rippeth, *Comparing the performance of the Mellor-Yamada and the κ-ε two-equation turbulence models.* Journal of Geophysical Research: Oceans, 1998. **103**(C5): p. 10543-10554.
53. Warner, J.C., et al., *Performance of four turbulence closure models implemented using a generic length scale method.* Ocean Modelling, 2005. **8**(1): p. 81-113.
54. Smagorinsky, J., *General circulation experiemnts with the primitive equations: I. The basic experiment.* Monthly Weather Review, 1963. **91**(3): p. 99-164.
55. Maar, M., et al., *Nutrient extraction and ecosystem impact by suspended mussel mitigation cultures at two contrasting sites.* Science of The Total Environment, 2023. **888**: p. 164168.
56. Maar, M., et al., *Ecosystem modelling across a salinity gradient from the North Sea to the Baltic Sea.* Ecological Modelling, 2011. **222**(10): p. 1696-1711.
57. Maar, M., et al., *The importance of local versus external nutrient loads for Chl a and primary production in the Western Baltic Sea.* Ecological Modelling, 2016. **320**: p. 258-272.
58. Neumann, T., et al., *Non-Redfieldian carbon model for the Baltic Sea (ERGOM version 1.2) – implementation and budget estimates.* Geosci. Model Dev., 2022. **15**(22): p. 8473-8540.
59. Windolf, J., et al., *A distributed modelling system for simulation of monthly runoff and nitrogen sources, loads and sinks for ungauged catchments in Denmark.* Journal of Environmental Monitoring, 2011. **13**(9): p. 2645-2658.
60. van Leeuwen, S. and H. Lenhart, *OSPAR ICG-EMO riverine database 2020-05-01 used in 2020 workshop*, S. van Leeuwen and H. Lenhart, Editors. 2021, NIOZ.
61. Lindström, G., et al., *Development and testing of the HYPE (Hydrological Predictions for the Environment) water quality model for different spatial scales.* Hydrology Research, 2010. **41**(3-4): p. 295-319.
62. Powers, J.G., et al., *The Weather Research and Forecasting Model: Overview, System Efforts, and Future Directions.* Bulletin of the American Meteorological Society, 2017. **98**(8): p. 1717-1737.
63. Skamarock, W.C., et al., *A Description of the Advanced Research WRF Version 3*, in *NCAR Technical Note, NCAR/TN-475+STR.* 2008. p. 27.

64. Fitch, A.C., et al., *Local and Mesoscale Impacts of Wind Farms as Parameterized in a Mesoscale NWP Model.* Monthly Weather Review, 2012. **140**(9): p. 3017-3038.
65. Fischereit, J., et al., *Review of Mesoscale Wind-Farm Parametrizations and Their Applications.* Boundary-Layer Meteorology, 2022. **182**(2): p. 175-224.
66. Siedersleben, S.K., et al., *Micrometeorological impacts of offshore wind farms as seen in observations and simulations.* Environmental Research Letters, 2018. **13**(12): p. 124012.
67. Smith, S.D. and E.G. Banke, *Variation of the sea surface drag coefficient with wind speed.* Quarterly Journal of the Royal Meteorological Society, 1975. **101**(429): p. 665-673.
68. Hendriks, E., et al., *The impact of offshore wind turbine foundations on local hydrodynamics and stratification in the Southern North Sea.* Frontiers in Marine Science, 2025. **Volume 12 - 2025**.
69. Pebesma, E. and R. Bivand, *Spatial Data Science: With Applications in R (1st ed.). Chapman and Hall/CRC. https://doi.org/10.1201/9780429459016*. 2023.
70. Larsen, J., *FlexSem source code. Zenodo. https://doi.org/10.5281/zenodo.15695485*. 2025.
71. Maar, M., et al., *FlexSem hydrodynamic-biogeochemical model North Sea [Software]. Zenodo. https://doi.org/10.5281/zenodo.15358807*. 2025.

Figure legends.

Figure 1. Offshore wind farm effects on hydrodynamics. The effects considered are a) the wind wake causing reduced wind stress at the sea surface, less mixing and stronger stratification of the water column and b) the drag effect from monopiles causing increased local mixing and less stratification of the water column. Hence, the two effects from offshore wind are causing opposite effects on water column mixing and stratification operating on different temporal-spatial scales.

Figure 2. The wake effect (wind speed) around the offshore wind farms. Annual difference in mean wind speed (m s^{-1}) between Y2030 and REF-NO-FARM for a) the North Sea and b) the Baltic Sea from the WRF model. The location of offshore wind farms is shown as black points.

Figure 3. **Stratification, current speed and primary production.** Yearly means of water column stratification index (J m^{-3}) (a, b), current speed (m s^{-1}) (c, d) and primary production (mg-C m^{-2} d^{-1}) for the North Sea and the Baltic Sea, respectively. Maximum PEA was 1019 J m^{-3} and 577 J m^{-3} for the North Sea (Skagerrak) and Baltic Sea (Kattegat), respectively. The location of offshore wind farms is shown as red points.

Figure 4. **Stratification index (PEA)**. Mean (±standard error, SE) responses of stratification index (%) with increasing distance (km) from the offshore wind farms (a, b) in the North Sea and the western Baltic Sea, respectively, yearly and during summer (April to September). Mean stratification index (J m^{-3}, 0-40 m) within a 40 km radius in the North Sea and 20 km radius in the Baltic Sea from offshore wind farm areas (c, d), and time-series responses of stratification index (%) to offshore wind farm development within the offshore wind farms (OWF) and within a radius of 40 km (North Sea) and 20 km (Baltic Sea) from the OWF (e, f).

Figure 5. **Primary production**. Mean (±SE) responses of primary production (PP, %) with increasing distances (km) from the offshore wind farms (a, b) in the North Sea and the western Baltic Sea,

respectively, yearly and during summer (April to September). Seasonal primary production (mg-C m^{-2} d^{-1}, 0-40 m depth) within a 40 km radius in the North Sea and 20 km radius in the Baltic Sea from offshore wind farms (c, d), and responses of primary production (%) to offshore wind farm development within the offshore wind farms (OWF) and within a radius of 40 km (North Sea) and 20 km (Baltic Sea) from the OWF (e, f).

Figure 6. **Spatial responses of stratification and primary production**. Yearly median responses of PEA (a, b) and primary production (c, d) to offshore wind farms for the North Sea and the Baltic Sea, respectively.

Figure 7. Summer PEA and primary production responses to wind speed and current speed inside the offshore wind farms. (a) Summer PEA response to offshore wind shown as a color scale (%) for wind speed change (y-axis) and mean surface current speed (x-axis). If PEA increases (more stratified), the symbol color is red and if PEA decreases (more mixed), the symbol color is blue according to the color bar. Current speeds >0.25 m s-1 indicate when monopile mixing effects are dominating over the wake effects. Note that the North Sea (848 triangles) and the Baltic Sea (296 circles) have different symbols for the offshore wind farm areas.

(b) Primary production response (y-axis) as a function of PEA response on the x-axis with symbol colors representing mean current speed (CS, m s-1). SD of PEA response (%) within each offshore wind farm area is shown for each box separated by the zero-responses. BS=Baltic Sea, NS=North Sea. There was a significant Pearson correlation between primary production response versus PEA response (black solid line: N=1144, R= -0.40, R2=0.16, $p<0.001$). Regression line: $Y = -0.20X + 0.76$. All the primary production responses (increase or decrease) are further analyzed for PEA responses (increase or decrease) in Figure 8.Figure 8. Time-series of PEA and primary production (PP) responses inside the offshore wind farm areas. Summer PEA and primary production were averaged for all wind farms areas according to the four outcomes in Figure 7b: a) Reduced summer PEA and increased summer primary production, b) reduced PEA and increased primary production, c) reduced PEA and reduced primary production, and d) increased PEA and reduced primary production.

Figure 8. Time-series of PEA and primary production (PP) responses inside the offshore wind farm areas. Summer PEA and primary production were averaged for all wind farms areas according to the four outcomes in Figure 7b: a) Decreased summer PEA and increased summer primary production, b) decreased PEA and increased primary production, c) decreased PEA and decreased primary production, and d) increased PEA and decreased primary production. The inserted subfigures show the extracted data area (red box) in Figure 7b.